Characterization of Ultrashort Laser Pulses

Monica Martinez de Azagra, Georg August Universität Göttingen, Germany

September 4, 2019

Abstract

Ultrashort laser pulses are the scientist's tool of choice when working within the range of nonlinear optics. This report gives a brief introduction to the method of frequency resolved optical gating (FROG) which is used to measure the pulse length and electrical field of a 2.1 μm laser. Furthermore, the beam diameter and the beam profile are characterized using the knife edge method and different InGaAs detectors. The obtained results are presented and discussed.

Contents

1 Introduction

Ultrashort laser pulses, i.e. pulses with a time duration which is usually shorter than a picosecond (10^{-12} s), are widely used in the field of nonlinear optics as the thus applied electric field to the material is strong enough to trigger nonlinear responses in selected materials.
Another important field of application is the use of ultrashort pulses as probing tools for time resolved measurements of ultrafast events. The motion of different structures and particles in the microcosm is spread out over the time axis as you can see in figure 1 and can range from hundreds of femtoseconds (10^{-15} s) for the motion of atoms in molecules and solids to a few attosenconds (10^{-18} s) for the electrons in atoms.
By implementing pump probe experiments using ultrashort pulses of the required length, these motions can be visualized .

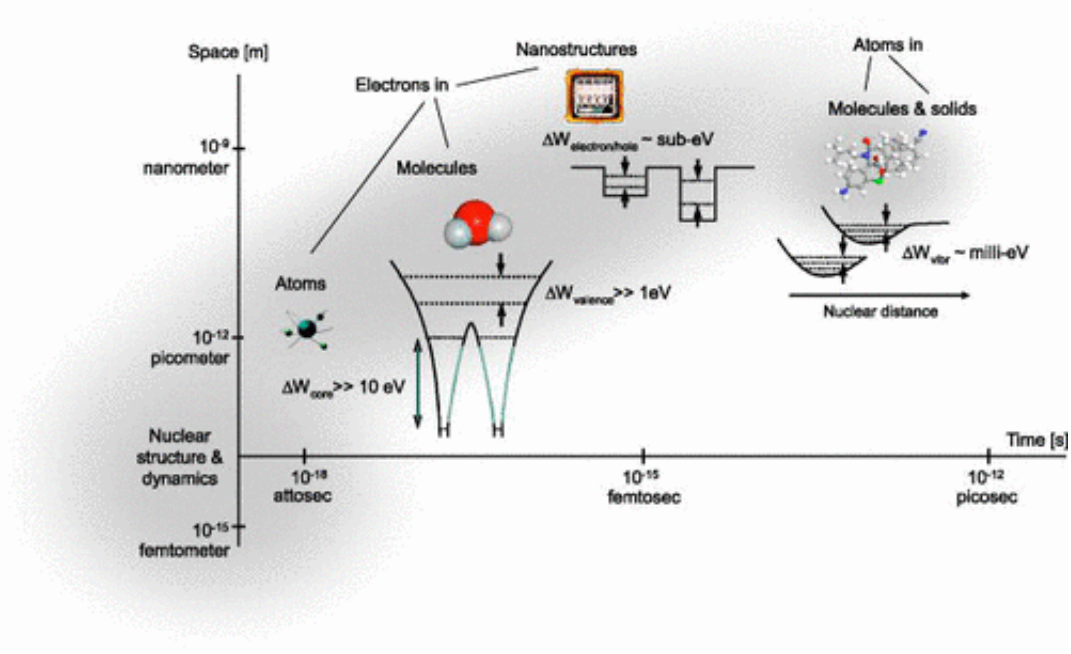

Figure 1: Visualization of the timescale on which the motion of different particles in the microcosm takes place. Taken from [1].

This report gives an account of the work done during my summer student internship in the group of Franz Kärtner at C-FEL at DESY in Hamburg. The goal for my time there was to characterize the ultrashort laser pulses of the Opera 2100 nm laser in time and space. To determine the duration of the laser pulses the method of frequency resolved optical gating (FROG) was used, a technique which enables precise knowledge of the pulse shape in time and frequency by extracting the electric field of the pulse through spectrally resolved autocorrelation. To measure the size of the pulses' intensity beam profile the knife edge technique was implemented and further test measurements were taken using a new beam profile detector developed previously in the group by Roland Mainz and Miguel Silva Toledo.

2 Theory

In the following section a brief introduction is given to the theoretical concepts of frequency resolved optical gating, a technique to measure both the electric field, the pulse shape and the length of ultrashort pulses, and the knife edge method to measure the diameter of a laser beam's intensity profile.

2.1 Frequency resolved optical gating

In section 1 it was noted that different pulse lengths enable the experimenter to probe dynamics on different time scales and that the shorter the laser pulses get, the faster the motion one can resolve. Therefore, the measurement of a pulse's length is crucial. The pulse length is strictly related to the chirp of the pulse i.e. the phase of the electric field. Hence, it is desirable to not only measure the length of the pulse but also to resolve the electric field.
Up to the 1980s the method of choice to measure the length of an ultrashort pulse were several methods using autocorrelation in the time or frequency domain, where you use a in time controlled delayed copy of your pulse $E(t-\tau)$ to scan over the pulse $E(t)$.

$$A(\tau) = \int_{-\infty}^{+\infty} E(t)\ E^*(t-\tau) \tag{1}$$

However, any of the experimental realizations of an optical autocorrelation in either the time (e.g. intensity, field autocorrelation) or the frequency domain (e.g. interferometric autocorrelation) fail to retrieve the complete electric field due to the fact that in some cases the problem yields an one-dimensional phase retrieval problem, which does not have a unique solution and in other cases the necessary retrieval algorithms don't converge, hence it is impossible to retrieve the exact electric field of a pulse.
Nonetheless, in 1991 Trebino et al. invented a technique that combines both measurements in the time and frequency domain and measures a spectrally resolved autocorrelation. This technique is called frequency resolved optical grating (FROG).
In figure 2 the general working scheme of a second harmonic generation (SHG) FROG

setup is depicted. A copy of a pulse is created with the help of a beam splitter and variably delayed in time before being focused together with the original pulse into a nonlinear crystal. The delay dependant second harmonic is then recorded with a spectrometer for every delay position τ.

The mathematical concept behind FROG is the spectrogram $\Sigma(\omega, \tau)$, i.e. the visual-

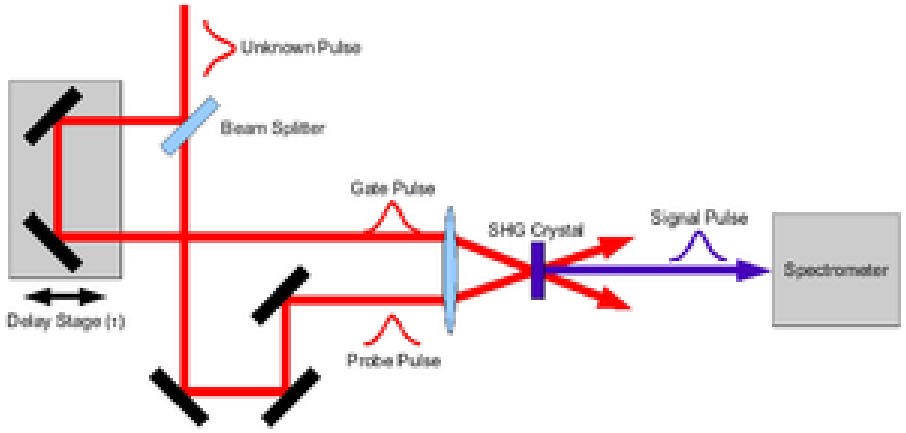

Figure 2: Schematic setup of a second harmonic FROG. A copy of a pulse is generated using a beam splitter. The copy is the send over a linear delay stage to be able to variate the time delay between the original and the copied pulse. Both pulses are then focused into a nonlinear crystal to generate the second harmonic. When the pulses overlap in time in the crystal a delay dependent second harmonic signal is generated which is then recorded with a spectrometer. Taken from [2].

ization of frequencies as a function of time:

$$\Sigma(\omega, \tau) = \left| \int_{-\infty}^{+\infty} E(t)\ g(t-\tau)\ \exp(-i\omega t)\ \mathrm{d}t \right|^2 , \tag{2}$$

with the variable delay gate function $g(t-\tau)$, and the electric field $E(t)$ of the pulse. The measurement of the spectrogram of a field $E(t)$ allows for the complete (with the exception of a few factors) determination of the electric field.

Unlike other autocorrelation techniques FROG measures the spectrum at each delay position. The measured signal which for a SHG FROG yields the Fourier transform of the autocorrelation $A(t, \tau)$

$$A(t, \tau) = E(t)\ E(t-\tau)\ , \tag{3}$$

to be

$$I(\omega, \tau) = \left| \int_{-\infty}^{+\infty} A(t, \tau)\ \exp(-i\omega t)\ \mathrm{d}t \right|^2 . \tag{4}$$

To obtain the electric field $E(t)$ the autocorrelation is written as the Fourier transform of a new function $A(t, \Omega)$, which is the Fourier transform of $A(t, \tau)$ with respect to Ω

$$A(t, \tau) = \int_{-\infty}^{+\infty} A(t, \Omega) \ \exp(-i\Omega\tau) \ \mathrm{d}\Omega \ . \tag{5}$$

This expression can now be substituted into equation 4 yielding the following equation for the measured spectrogram

$$I(\omega, \tau) = \left| \int_{-\infty}^{+\infty} \int_{-\infty}^{+\infty} A(t, \Omega) \ \exp(-i\omega t - i\Omega\tau) \ \mathrm{d}t \ \mathrm{d}\Omega \right|^2 . \tag{6}$$

Equation 6 represents a two-dimensional phase retrieval problem which can be solved yielding a unique solution for $A(t, \Omega)$.
$A(t, \Omega)$ in turn is the inverse Fourier transform of $A(t, \tau)$, which is related to the electric field $E(t)$

$$A(t, \tau = t) = E(t) \ E(0) \approx E(t) \ , \tag{7}$$

where the constant factor $E(0)$ can be neglected.
Therefore, by measuring the spectrogram 6 and using a suitable phase retrieval algorithm the electric field of a pulse can be determined.

2.2 The knife edge method

To estimate peak intensities of pulsed lasers it is necessary to know the size of the beam at the position of interest, e.g. the focal point of a lens. An established technique to measure the size of a laser beam in the focus, is to take a razor knife, move it with micrometer precision through the beam profile (see figure 3) and record the intensity as a function of the position x of the knife.

This method is known as the knife edge method and yields the intensity profile of the pulse at measured position z along the beam propagation axis. Assuming a symmetric Gaussian intensity distribution for the beam profile, the intensity distribution of the beam profile is given by

$$I(x, y) = I_0 \cdot \exp\left(\frac{-2x^2}{w^2}\right) \cdot \exp\left(\frac{-2y^2}{w^2}\right) \ , \tag{8}$$

with the beam diameter w, and the amplitude I_0. The total intensity P_{tot} of the beam profile in two dimensions amounts to

$$\begin{aligned} P_{tot} &= I_0 \int_{-\infty}^{+\infty} \exp\left(\frac{-2x^2}{w^2}\right) \mathrm{d}x \int_{-\infty}^{+\infty} \exp\left(\frac{-2y^2}{w^2}\right) \mathrm{d}y \\ &= I_0 \frac{\pi}{2} w^2 \ . \end{aligned} \tag{9}$$

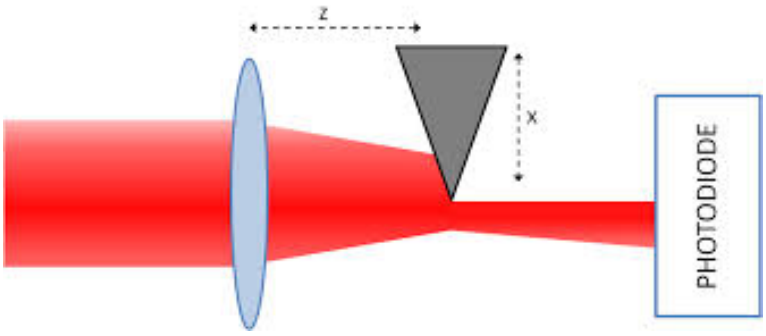

Figure 3: Working scheme of the knife edge method. A knife edge is positioned on xz-delay stage. By moving it along the x-axis of the beam profile the intensity of the as function of x (see equation 10) is recorded with a photodiode. By rpeating this measurement along the z-axis on can determine the evolution of the beam diameter with equation 11 Taken from [3].

To determine the intensity $P(x)$ when the knife edge is at position x, the integral in x-direction changes to

$$\begin{aligned}
P(x) &= \int_{-\infty}^{+\infty}\int_{-\infty}^{x} I_0 \exp\left(\frac{-2x^2}{w^2}\right)\exp\left(\frac{-2y^2}{w^2}\right)\mathrm{d}x\ \mathrm{d}y \\
&= I_0\sqrt{\frac{\pi}{2}}w\int_{-\infty}^{x}\exp\left(\frac{-2x^2}{w^2}\right)\mathrm{d}x \\
&= I_0\sqrt{\frac{\pi}{2}}w\left[\int_{-\infty}^{0}\exp\left(\frac{-2x^2}{w^2}\right)\mathrm{d}x + \int_{0}^{x}\exp\left(\frac{-2x^2}{w^2}\right)\mathrm{d}x\right] \\
&= I_0\sqrt{\frac{\pi}{2}}w\left[\frac{1}{2}\sqrt{\frac{\pi}{2}}w + \int_{0}^{x}\exp\left(\frac{-2x^2}{w^2}\right)\mathrm{d}x\right] \\
&= \frac{I_0}{2}\frac{\pi}{2}w^2 + I_0\sqrt{\frac{\pi}{2}}w\cdot\int_{0}^{x}\exp\left(\frac{-2x^2}{w^2}\right)\mathrm{d}x \\
&= \frac{P_{tot}}{2}\left[1+\mathrm{erf}\left(\frac{\sqrt{2}x}{w}\right)\right]\ . \qquad (10)
\end{aligned}$$

By measuring the intensity of the beam profile along one of its major axes, the beam diameter w can be determined by fitting equation 10 to the measured intensities $P(x)$ by means of regression analysis.
The evolution of the size of the diameter of a Gaussian beam $w(z)$ along its propagation axis z is described by equation 11

$$w(z) = \sqrt{1+(z/z_R)^2}\ , \qquad (11)$$

with the Rayleigh length z_R

$$z_R = \frac{\pi w_0^2}{\lambda} \qquad (12)$$

which yields the distance over which the beam can propagate without diverging significantly and depends on the minimal beam diameter w_0 and the wavelength λ of the laser.

3 Measurement

In the following section the results obtained to characterize the laser pulses of the Opera 2100 in time and space are presented. First, the FROG technique was used to characterize the pulse length and retrieve the electric field of the pulse, then the knife edge method was implemented to measure the beam diameter at the focal point. Lastly a, in the group newly developed, beam profile detector was used to record the beam's intensity profile and to compare it to the knife edge measurements.

3.1 Pulse length measurements with FROG

To measure the pulse length in the time domain and the electric field of the pulses of the Opera 2100 nm the beam was coupled into a FROG setup based on the scheme in figure 2 and recorded with a HR4000 spectrometer. A 100 μm BBO was used to generate the second and third harmonic of the fundamental at 2.1 μm. The spectrum of the fundamental wavelength was recorded with a NIRQuest spectrometer. The measurements were recorded with a preexisting Labview program and evaluated with the FROG retrieval software from Femtosoft.

Second harmonic FROG

In a first step the time dependent second harmonic is found by detecting the interference pattern that can be seen in the spectrometer as the delay stage is moved over the point where both pulses overlap in time (as well as in space). After finding the temporal overlap the spectrum is recorded every 1 fs delay step yielding a spectrogram of the form of equation 6. The results are depicted in figure 4a.
The FROG trace is as expected for a SHG FROG symmetric along time zero, and the retrieved FROG trace matches the measurements well. The pulse shape is not Gaussian but shows three peaks. Nonetheless, at full-width half maximum the pulse length is measured to be 59 fs. The temporal phase is constant over the length of the pulse which indicates there to be no chirp. However, there is a large discrepancy of roughly 50 nm between the reconstructed and the measured spectrum of the fundamental.
The second harmonic is expected to be at approximately 1050 nm, which is at the edge of the sensitivity of the spectrometer REF. Figure 4b shows a comparison of the spectra of the second and third harmonics multiplied by their respective order recorded with different spectrometers. The spectrum of the second harmonic is shifted by roughly 70 nm in the same direction as the reconstructed FROG spectrum in figure 4a. The third harmonic recorded with the HR4000 spectrometer as well as the USB2000 also

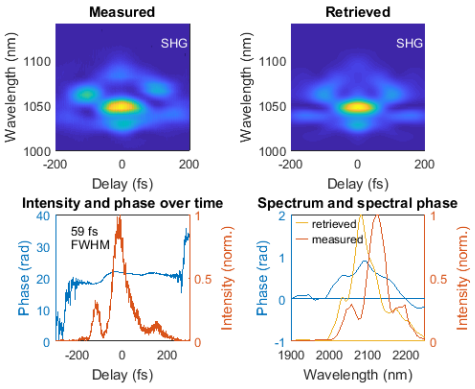

(a) FROG measurements for a SHG FROG from top to bottom: measured and retrieved FROG trace, pulse length and reconstructed and measured spectrum of the fundamental.

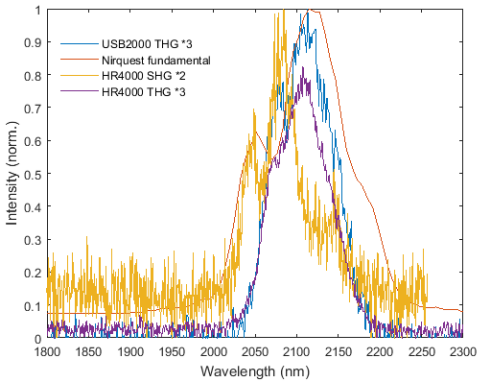

(b) The fundamental wavelength and its second and third harmonics were recorded with different spectrometers and plotted on the same graph by multiplying the harmonics with their respective order. The graph shows a distinctive spectral shift of the second harmonic.

Figure 4: The results for the non calibrated SHG FROG measurements and the comparative measurements of different spectromters.

shows a slight shift of the peaks relative to the fundamental, however the shift is much smaller comapred to the seciond harmonic.
Even though the second harmonic lies at the very edge of the sensitivity of the HR4000 spectrometer, both of these discrepancies can be evaded by multiplying the measured spectra by the calibration factors (see figure 5b). The results for the calibrated SHG FROG measurements are depicted in figure 5a. Compared to figure 4a the intensities are magnified through the multiplication of the calibration factors (the resulting noise could succesfully be diminished using post measurement filtering techniques). The retrieved FROG trace matches the measurements as well as the reconstructed spectrum. The pulse length at FWHM is 70 fs, which can be assumed to be the correct pulse length as the spectral reconstruction matches the measured spectrum and the retrieved trace matches the measurement.

Third harmonic FROG

As a means of comparison the FROG measurement was repeated using the third harmonic. The results are depicted in figure 6. The retrieved and measured FROG traces coincide in their approximate shape, whilst the retrieved trace is less defined. The pulse shape is the same as in figure 5 with small variations. While for the second harmonic FROG the retrieved and the measured spectrum matched perfectly the reconstructed spectrum of the third harmonic FROG has a second main peak shifted to the left from

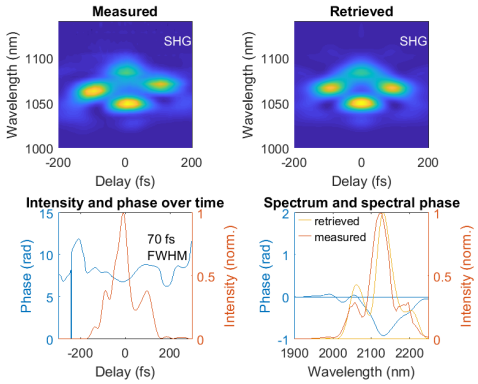

(a) FROG measurements for a SHG FROG from top to bottom: measured and retrieved FROG trace, pulse length and reconstructed and measured spectrum of the fundamental.

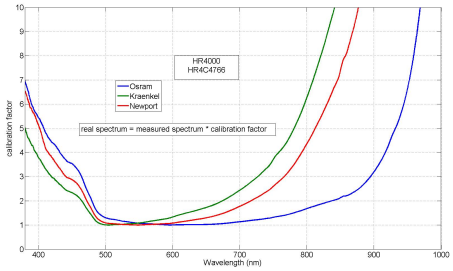

(b) Calibration factors for the HR4000 spectrometer.

Figure 5: Spectrally calibrated SHG FROG measurements and the calibration factors for the HR4000 spectrometer used to measure the FROG traces.

the actual main peak of the measured spectrum. However, this does not change the results significantly. The measured pulse length for THG FROG is 73 fs.

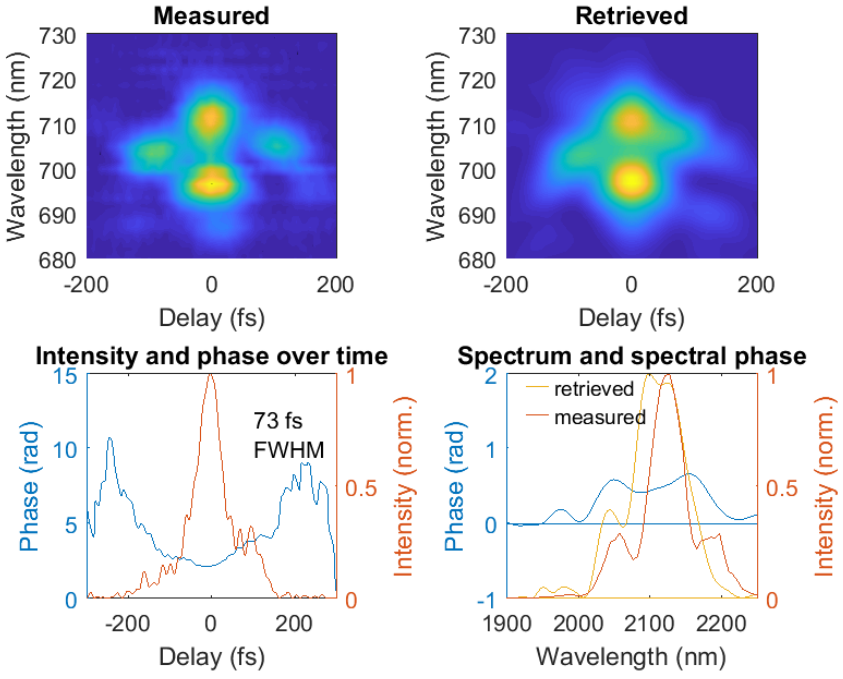

Figure 6: FROG Measuremnts for third harmonic generation.

3.2 Knife edge method

One of the goals of this work was to measure the beam diameter at the focal point of the setup used to obtain the results in REF NICOS PAPER. To measure the beam diameter a knife edge was positioned on a micrometer xz-stage module (as seen in figure 3) and placed into the beam path at the position of the expected focal point.
Several measurements of the beam diameter were taken along the propagation axis of the beam to be able to determine the diameter at the focal point of the lens used in the setup. By means of linear regression equation 10 was fitted to the measured intensities $P(x, z)$ and plotted in figure 7a.

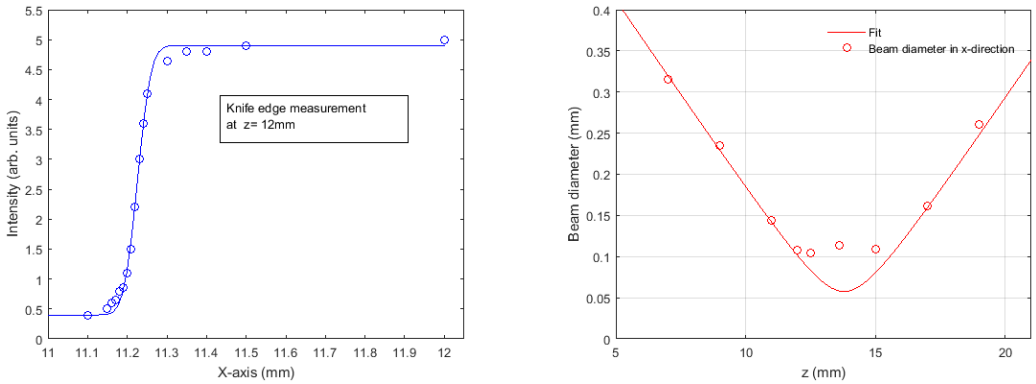

(a) Intensity measurement of the beam profile fitted with equation 10 at the position z = 12 mm.

(b) Plot of the evolution of the beam diameter along the propagation axis of the beam, fitted to function 11.

Figure 7: Exemplary Knife edge measurement evolution of the beam diameter.

The parameters determined through regression analysis of equation 10 yield the required beam diameter w.
To obtain the beam's diameter at the focal point the values for the beam diameter at every position of measurement z were plotted and fitted with equation 11 by means of regression analysis in figure 7b.
One can see in figure 11 that the values for the beam diameter don't align with the line of equation 11 at the designated focal point in figure 7b, and instead stay on a constant plateau, where one would expect to be a minimum.

To further investigate this deviation, a beam profile camera was used to visualize the shape of the beam profile of the collimated beam (see figure 8). The collimated beam shows a flat top beam intensity profile. By applying the Fourier transform one obtains the beam profile at the position of the focal point, which yields a sinc^2 function (see figure 8b).
The flat top beam distribution of the beam's intensity profile and the corresponding sinc^2 function intensity distribution at the focal point means the initial assumption of a Gaussian pulse for equation 10 is faulty as well as the equation for the propagation 11

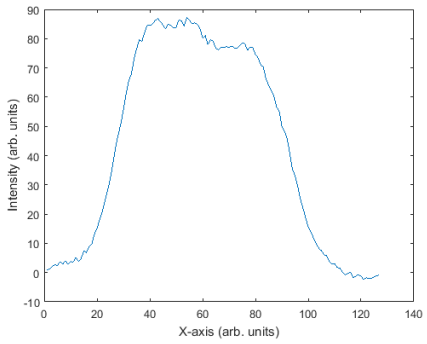

(a) Averaged intensity distribution of the beam profile of the collimated beam along the x-axis measured with beam profile camera.

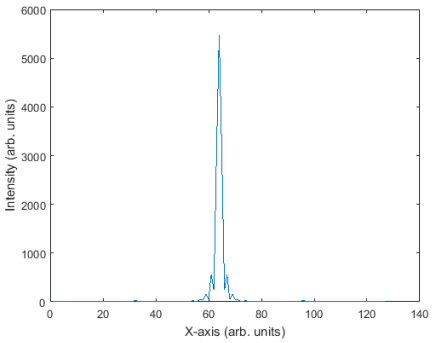

(b) Fourier transformed intensity distribution of the collimated beam in figure 8b.

Figure 8: Intensity distribution of the beam profile along the x axis for collimated and focused beam.

of the beam diameter. Nevertheless, the approximation fits the measurements outside the focal point yielding some usefullness.

3.3 Beam profile detector

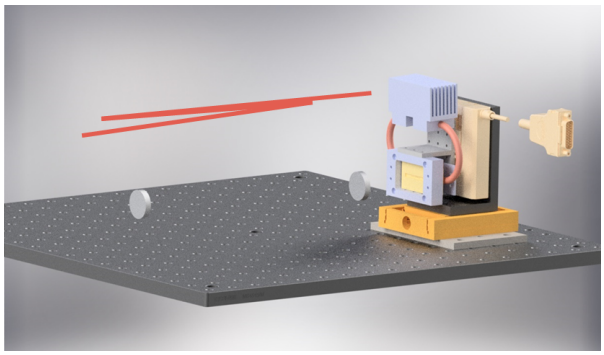

(a) CAD scheme of the detector. Image provided by Miguel Silva Toledo.

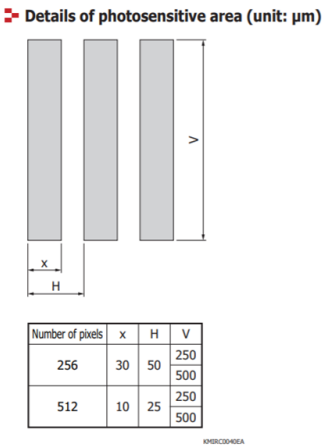

Number of pixels	x	H	V
256	30	50	250
			500
512	10	25	250
			500

(b) Sketch of the detector plane. The detector consists ofan array of 256 InGaAs CCDs. Image provided by Miguel Silva Toledo.

Figure 9: Details on the beam profile detector.

To compare the measurements taken with the knife edge method, further measurements were done with an InGaAs beam profile detector, which had previously been build in the group.
The detector consists of an array of 256 InGaAs CCDs (see figure 9) which are moved in y-direction to scan through the beam profile. The measurement is repeated along the propagation axis of the beam to evaluate the beam diameter at the focal point of the lens. Figure 10 shows the evolution of the beam profile before and approximately at the focal point.

Evaluation of the data in x-direction yields the intensity profile as it has been determined prior with the knife edge method. By means of regression analysis a Gaussian (see figure **??**) is fitted to the averaged intensities along the x-axis. The resulting beam diameter at every position is plotted in figure 12 and fitted to equation 11.
As in figure 7b one observes that the propagation of the beam diameter does not follow the Gaussian beam evolution from equation 11. The expected the sinc^2 intensity distribution at the focal point could not be resolved with the beam profiler.
The resolution limit of the detector in x-direction is $50\,\mu$m, the width of the one CCD. Therefore, the smallest beam diameter one could measure would be $50\,\mu$m. Therefore, the detector is not sensitive enough in x-direction to be able to resolve the expected sinc^2 function intensity profile at the focal point.
The resolution in y-direction should be limited by the step size of the delay stage the

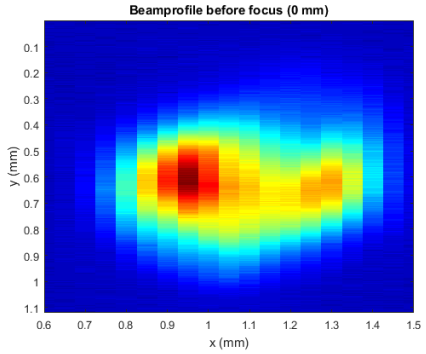

(a) Beam profile recorded at position z = 0 before the focal point.

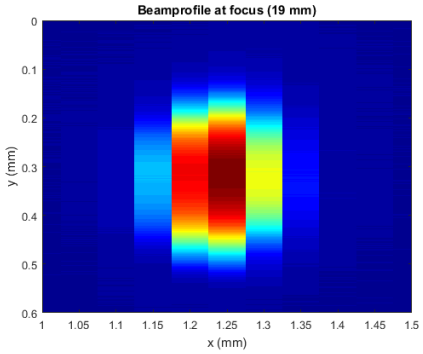

(b) Beam profile at near the focal point at position z = 19 mm.

Figure 10: Beam profile measurements wit the beam profile detector.

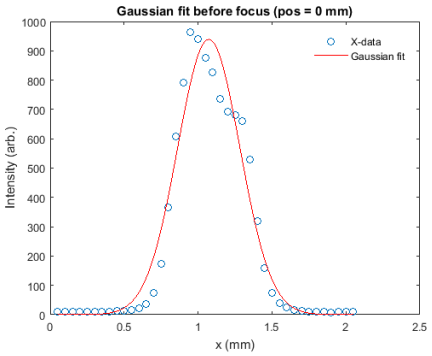

(a) The averaged intensity distribution along the x-axis in figure 10a was plotted and fitted to a Gaussian.

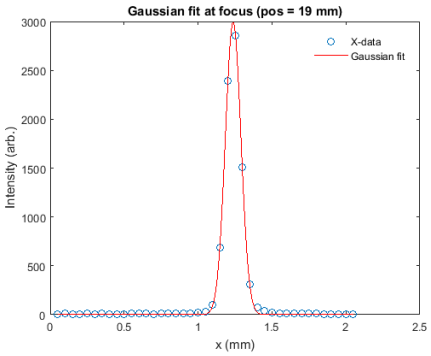

(b) The averaged intensity distribution along the x-axis in figure 10b was plotted and fitted to a Gaussian.

Figure 11: Plotted averaged intensity distributions before and at focal point plotted and fitted to a Gaussian.

detector is mounted on and the repetition rate of the laser. However, the final information retrieval presents a signal processing problem that I did not have the time to solve during my internship.

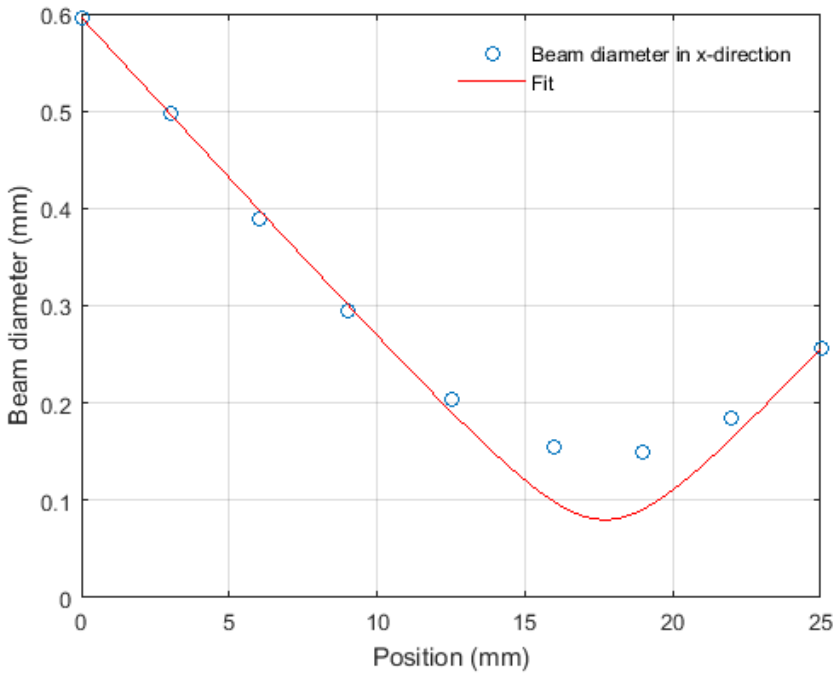

Figure 12: Evolution of the beam diameter measured with the beam profile detector and fitted to equation 11.

4 Conclusion

This report summarizes the results I achieved during my time at DESY. The duration of the pulses of the Opera 2100 laser were successfully measured to be 70 fs with the technique of frequency resolved optical gating.
Furthermore, the beam diameter was measured using the knife edge method and a beam profile detector, giving similar results. The result of the knife edge method yielding a beam diameter of 110 μm can be taken to be the more acurate measurement as it is not limited by the 50 μm resolution of the beam profile detector.

5 So long, and thanks for all the fish

At this point I would like to take the opportunity to thank DESY for letting me attend the summer school and Franz Kärtner and Oliver Mücke for the opportunity to work in their group. I especially want to thank Nicolai Klemke for supervising me and helping me along. I would also like to thank all the group members that I met for the great conversations, it was nice meeting so many interesting people.
I had a great time this summer at DESY!

References

[1] Ferenc Krausz and Misha Ivanov. *Attosecond physics*. Rev. Mod. Phys., 81(1):163234, 2009.

[2] Wikipedia: Frequency resolved optical gating, `https://en.wikipedia.org/wiki/Frequency-resolved`$_{o}ptical_{g}ating/media/File$: $SHG_{F}ROG.png$

[3] Practical instructions, `http://people.fjfi.cvut.cz/blazejos/public/ul7en.pdf`

[4] Rick Trebino. *Frequency-Resolved Optical Gating: The Measurement of ultrashort laser pulses*. Springer US, 2000.